

Search for displaced vertices of oppositely charged leptons from decays of long-lived particles in pp collisions at $\sqrt{s} = 13$ TeV with the ATLAS detector

Reinterpretation material

This document explains how the results of this search can be reinterpreted in others models that predict long-lived particles (LLPs) with a lifetime of ps to ns and a mass $m > 12$ GeV decaying into an oppositely charged ee , $e\mu$, or $\mu\mu$ pair. The overall signal efficiency S , defined as the fraction of events passing the selection criteria of the signal region, can be expressed in terms of the acceptance \mathcal{A} and the detection efficiency ϵ , i.e. $S = \mathcal{A} \times \epsilon$. The following two sections explain how to calculate the per-decay acceptance and efficiency for a new model. For models with multiple LLPs per event, it is assumed that the acceptances of the LLPs are independent of each other. The third section discusses the calculation of the corresponding per-event variables that take into account the number of LLPs per event and the branching ratios of the LLP decay. Finally, the exclusion of new signal models is discussed.

Acceptance

For the calculation of the acceptance, the selection criteria of the signal region are applied to the final-state particles of the Monte Carlo (MC) truth record. An event has to pass the following event-level requirements:

- There is no ee , $e\mu$, or $\mu\mu$ pair with $\sqrt{(|\Delta\phi| - \pi)^2 + (\eta_1 + \eta_2)^2} < 0.01$ (cosmic-ray veto). All final-state leptons of the event have to be used to evaluate this cut.
- The z position of the pp collision must satisfy $|z| < 200$ mm.
- There is at least one LLP decay that passes the requirements described below.

The following vertex-level requirements are applied to LLP decays:

- The LLP decay position must be within the fiducial volume of $r_{xy} < 300$ mm and $|z| < 300$ mm.
- The transverse distance between the pp collision and the LLP decay position must be greater than 2 mm.
- For each charged LLP decay product, the magnitude $|d_0|$ of its transverse impact parameter must be greater than 2 mm and its p_T must be greater than 1 GeV. All charged LLP decay products that fail at least one of the two cuts must be removed before the remaining requirements are evaluated. In addition, the mass of each charged LLP decay product must be set to the pion mass $m(\pi) = 139.57$ MeV to simulate the assumptions in the displaced vertex reconstruction used in the analysis.
- The invariant mass of the charged LLP decay products must be larger than 12 GeV.

- $N(e) + N(\mu) > 1$, where only electrons (muons) with $p_T > 10$ GeV and $|\eta| < 2.47$ (2.5) are considered.
- At least one of the following criteria must be satisfied:
 - One e with $p_T > 150$ GeV and $|\eta| < 2.47$
 - Two e with $p_T > 55$ GeV and $|\eta| < 2.47$
 - One μ with $p_T > 62$ GeV and $|\eta| < 1.07$
- There must be at least one positively charged and at least one negatively charged electron/muon.

The transverse impact parameter of a charged particle from a LLP decay can be calculated via

$$d_0 = d_{xy} \times \sin \Delta\phi, \quad (1)$$

where d_{xy} is the transverse distance between the pp collision and the LLP decay position and $\Delta\phi$ is the azimuthal angle between the particle momentum at its creation and the distance vector from the pp collision to the LLP decay.

A LLP decay is accepted if it passes the vertex-level cuts and the event passes the event-level cuts. Each accepted LLP is assigned a weight

$$w_{\text{LLP}} = (1 - w_{\text{Pix}}) \times (1 - w_{\text{Mat}}), \quad (2)$$

where w_{Pix} is obtained from Fig. 1(b) and w_{Mat} is obtained from Fig. 1(a) for LLP decays to ee or $e\mu$ and $w_{\text{Mat}} = 0$ for LLP decays to $\mu\mu$. The per-decay acceptance for the dilepton channel $\ell\ell'$ is given by

$$\mathcal{A}(\ell\ell') = \frac{\sum_{\text{accepted LLP decays to } \ell\ell'} w_{\text{LLP}} \times w_{\text{gen}}}{\sum_{\text{all LLP decays to } \ell\ell'} w_{\text{gen}}}, \quad (3)$$

where w_{gen} is the event weight calculated by the MC generator. The sums over LLPs imply sums over events.

Figure 2 shows per-decay acceptances for the RPV SUSY model and four combinations of squark and neutralino masses. They can be used to validate the implementation of the selection criteria.

Detection efficiency

Two parameterizations of the detection efficiency are provided. The first parameterization is derived from the RPV SUSY model, while the other parameterization is derived from the Z' toy model. The parametrization should be chosen based on the properties of the LLP decay of the target model. There are two major differences in the kinematics of the LLP decay between the two models. First, the LLP has on average a much higher p_T in the RPV SUSY model due to the large mass difference between the squark and the neutralino. Especially when the neutralino mass is only 50 GeV, the angle between the two charged leptons becomes very small, while in the Z' toy model many lepton pairs have $|\Delta\phi| \approx \pi$ even for $m(Z') = 100$ GeV. Furthermore, the r_{xy} and $|z|$ position of the LLP decay is larger on average in the RPV SUSY model (assuming the same LLP lifetime in both models) due to the larger Lorentz boost. The second major difference is that in the RPV SUSY model, the LLP decays not only to a pair of charged leptons, but also to a neutrino. Due to the neutrino momentum, the displacement vector pointing from the

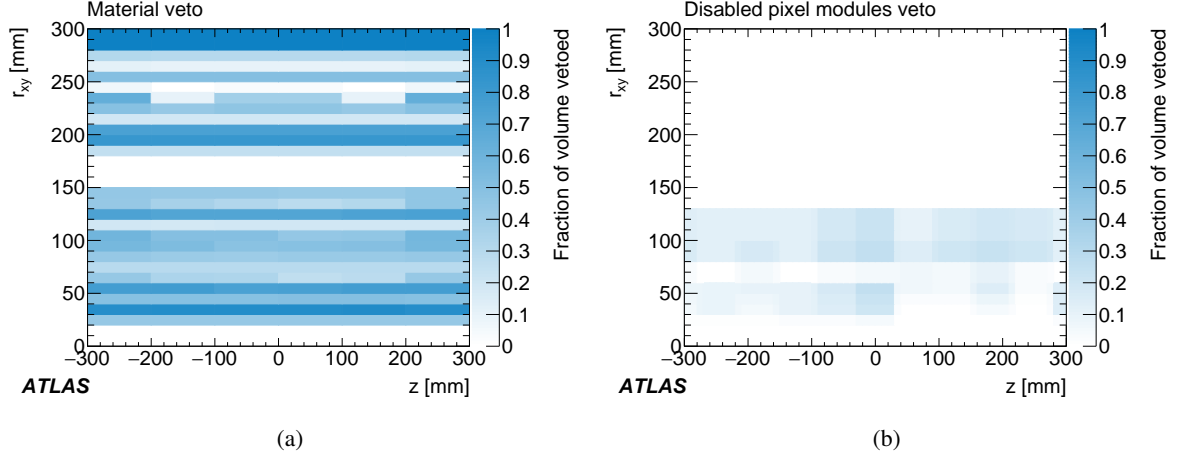


Figure 1: Fraction of detector volume covered by (a) the material veto and (b) the disabled pixel modules veto as a function of z and r_{xy} of the displaced dilepton vertex.

proton–proton collision to the LLP decay position is often not parallel to the momentum of the lepton pair, in contrast to the Z' toy model. All these differences have a non-negligible impact on the detection efficiency.

Figures 3 to 5 show the per-decay detection efficiencies for the RPV SUSY model, while Figures 6 to 10 show them for the Z' toy model. Both parameterizations are derived separately for each dilepton type and are binned in the transverse radius r_{xy} of the LLP decay and the invariant mass and p_T of the lepton pair. For most MC samples, the overall signal efficiency S derived with these parameterizations agrees with the nominal S within 20% for the RPV SUSY model and 10% for the Z' toy model.

The per-decay overall signal efficiency for the dilepton channel $\ell\ell'$ is given by:

$$S(\ell\ell') = \frac{\sum_{\text{accepted LLP decays to } \ell\ell'} \epsilon_P(\ell\ell', r_{xy}, m, p_T) \times w_{\text{LLP}} \times w_{\text{gen}}}{\sum_{\text{all LLP decays to } \ell\ell'} w_{\text{gen}}}, \quad (4)$$

where ϵ_P is obtained from one of the two parameterizations.

Per-event variables

Based on the per-decay variables, the corresponding per-event variables can be calculated that take into account the number of LLPs per event and the branching ratios of the LLP decay. If there is one LLP per event, the per-event variable X_{evt} ($= \mathcal{A}_{\text{evt}}$ or \mathcal{S}_{evt}) is given by:

$$X_{\text{evt}} = \mathcal{B}(ee) \times X(ee) + \mathcal{B}(e\mu) \times X(e\mu) + \mathcal{B}(\mu\mu) \times X(\mu\mu), \quad (5)$$

where \mathcal{B} is the branching ratio of the LLP decay and X the per-decay variable for one of the three dilepton channels. For two LLPs per event, the following equation has to be used:

$$\begin{aligned} X_{\text{evt}} = & \mathcal{B}(ee)^2 \times (1 - (1 - X(ee))^2) + \mathcal{B}(e\mu)^2 \times (1 - (1 - X(e\mu))^2) + \mathcal{B}(\mu\mu)^2 \times (1 - (1 - X(\mu\mu))^2) \\ & + 2 \times \mathcal{B}(ee) \times \mathcal{B}(e\mu) \times (1 - (1 - X(ee))(1 - X(e\mu))) \\ & + 2 \times \mathcal{B}(ee) \times \mathcal{B}(\mu\mu) \times (1 - (1 - X(ee))(1 - X(\mu\mu))) \\ & + 2 \times \mathcal{B}(e\mu) \times \mathcal{B}(\mu\mu) \times (1 - (1 - X(e\mu))(1 - X(\mu\mu))). \end{aligned} \quad (6)$$

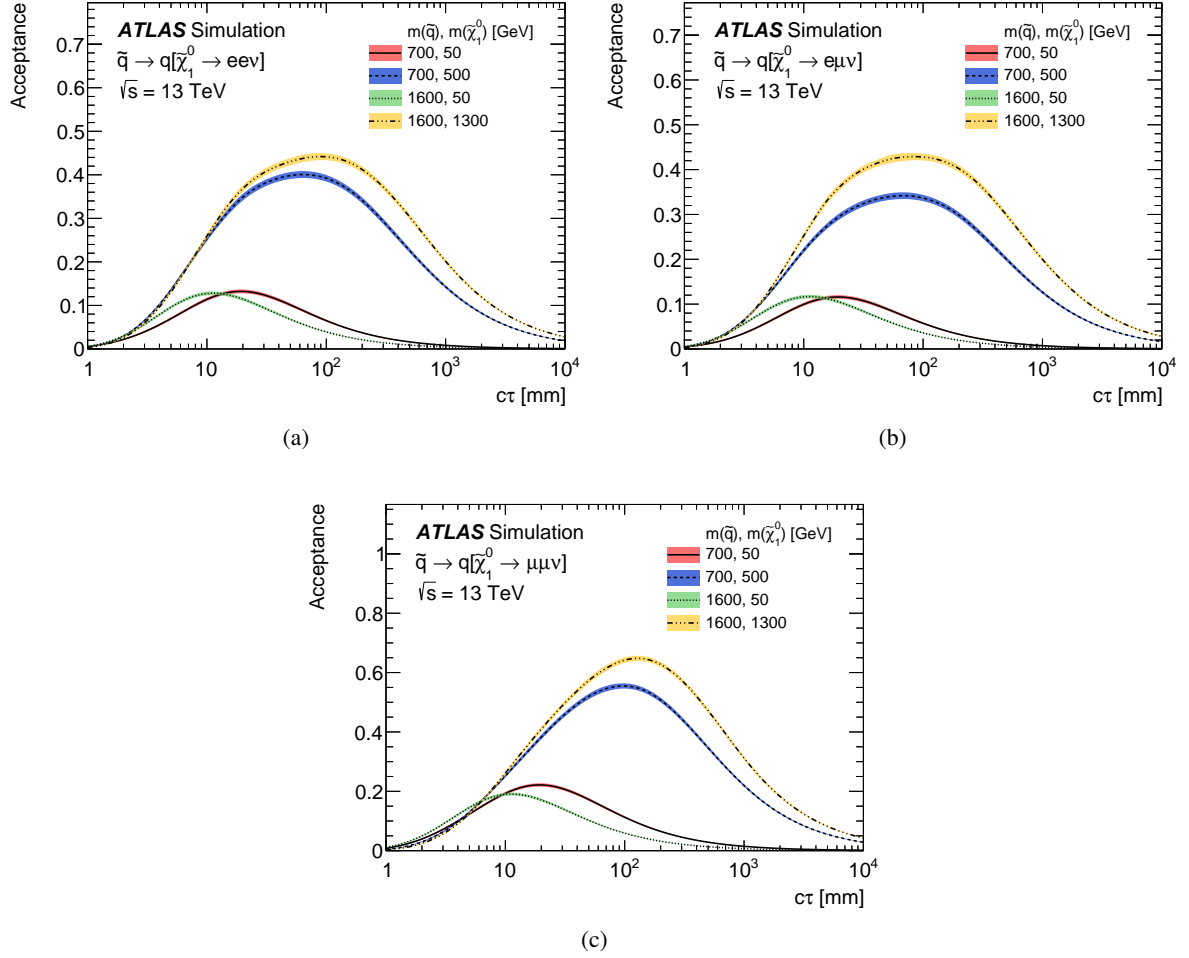
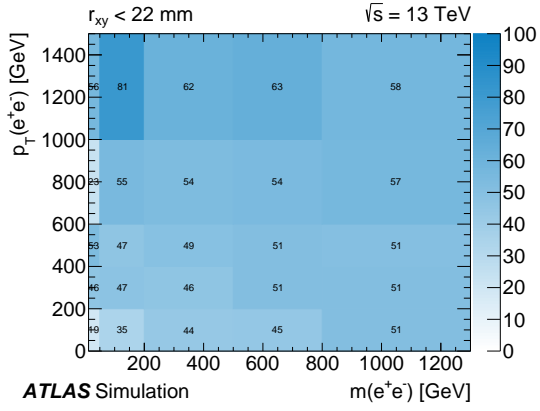
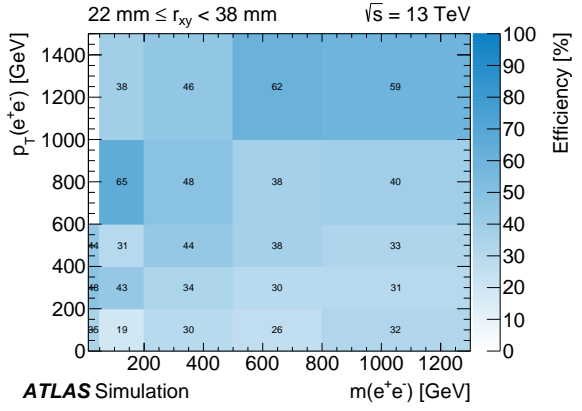


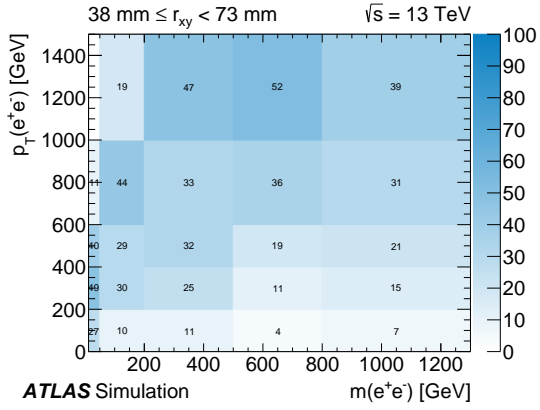
Figure 2: Acceptance \mathcal{A} per decay as a function of the mean proper lifetime of the $\tilde{\chi}_1^0$, in units of $c\tau$, for (a) $\tilde{\chi}_1^0 \rightarrow e e \nu$, (b) $\tilde{\chi}_1^0 \rightarrow e \mu \nu$, and (c) $\tilde{\chi}_1^0 \rightarrow \mu \mu \nu$ with various combinations of squark and $\tilde{\chi}_1^0$ masses. The shaded band indicates the statistical uncertainty.



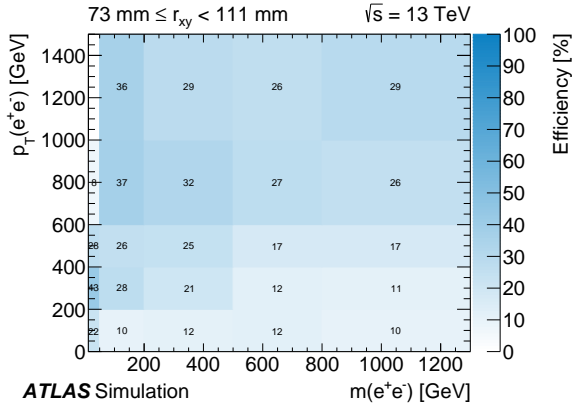
(a) $r_{xy} < 22$ mm



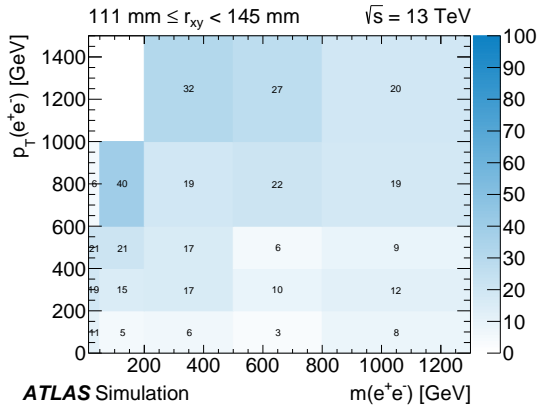
(b) $22 \text{ mm} \leq r_{xy} < 38$ mm



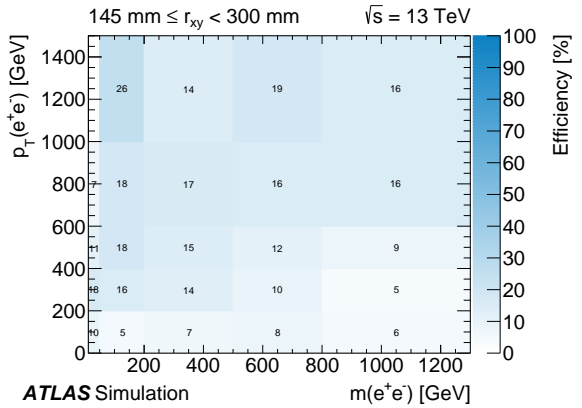
(c) $38 \text{ mm} \leq r_{xy} < 73$ mm



(d) $73 \text{ mm} \leq r_{xy} < 111$ mm



(e) $111 \text{ mm} \leq r_{xy} < 145$ mm



(f) $145 \text{ mm} \leq r_{xy} < 300$ mm

Figure 3: Detection efficiency ϵ per decay for various r_{xy} as a function of the invariant mass and p_T of the electron pair in $\text{LLP} \rightarrow e^+e^-X$.

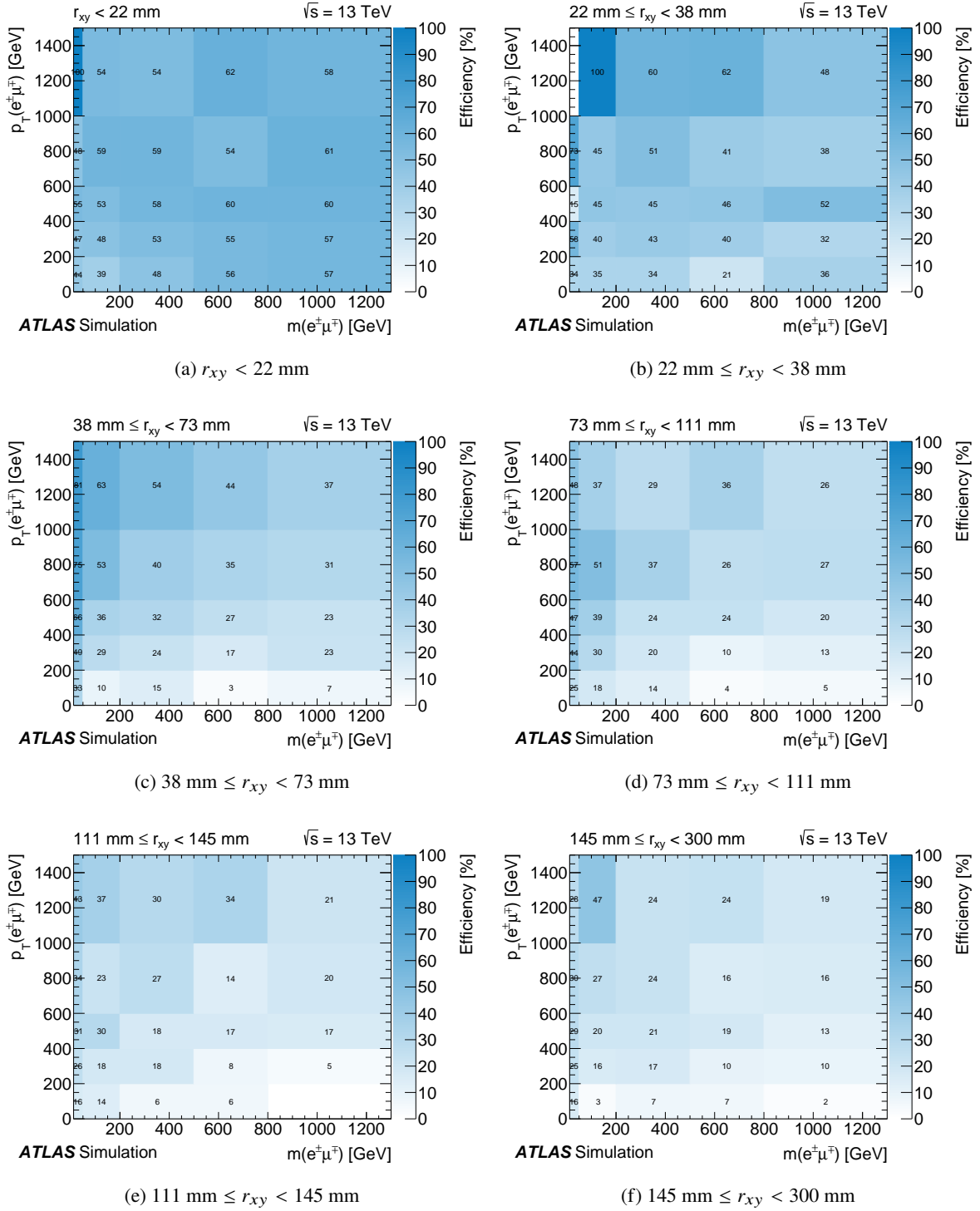


Figure 4: Detection efficiency ϵ per decay for various r_{xy} as a function of the invariant mass and p_T of the electron and muon pair in $LLP \rightarrow e^+\mu^- X$.

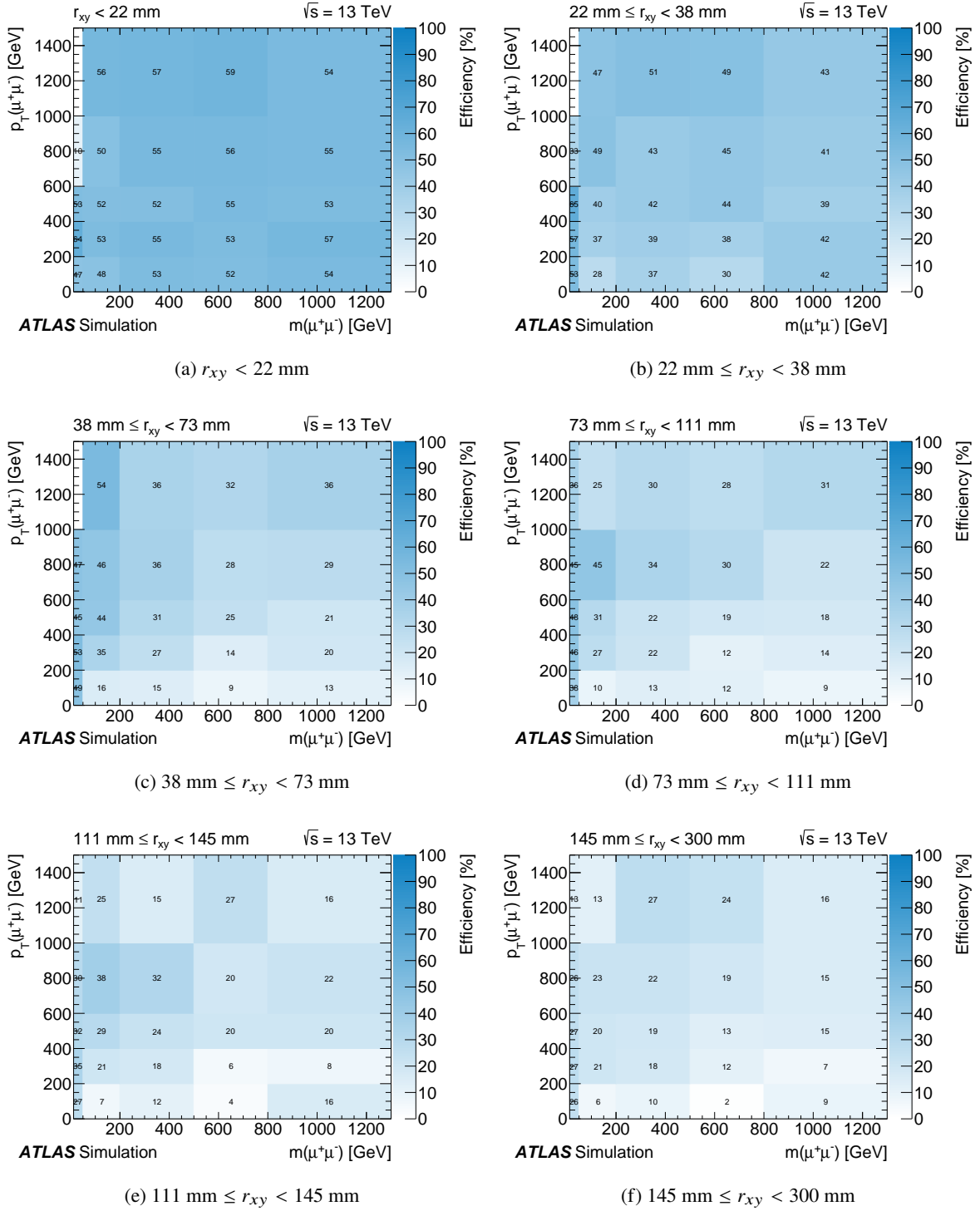


Figure 5: Detection efficiency ϵ per decay for various r_{xy} as a function of the invariant mass and p_T of the muon pair in LLP $\rightarrow \mu^+\mu^-X$.

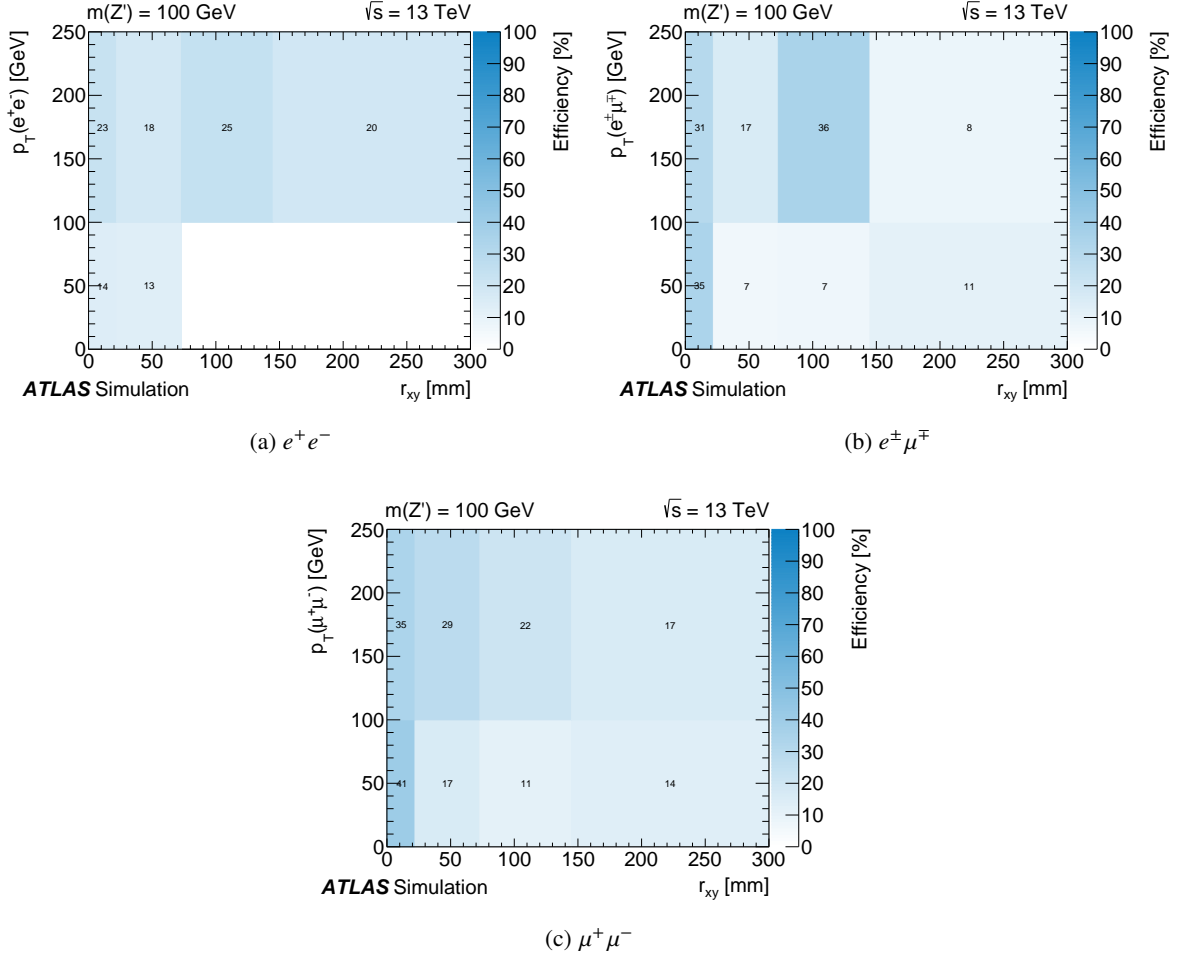


Figure 6: Detection efficiency ϵ per decay as a function of the transverse decay radius r_{xy} and the dilepton p_T for a LLP mass of 100 GeV and (a) $\text{LLP} \rightarrow e^+e^-$, (b) $\text{LLP} \rightarrow e^\pm\mu^\mp$, and (c) $\text{LLP} \rightarrow \mu^+\mu^-$.

Model exclusion

The number of expected signal events is given by:

$$N_{\text{Sig}} = S_{\text{evt}} \times \sigma \times L, \quad (7)$$

where σ is the production cross-section of the target model and $L = 32.8 \text{ fb}^{-1}$ the integrated luminosity. If this number is larger than the model-independent 95% CL upper limit on N_{Sig} of 3.0 events, then the model is expected to be excluded at 95% CL by this search.

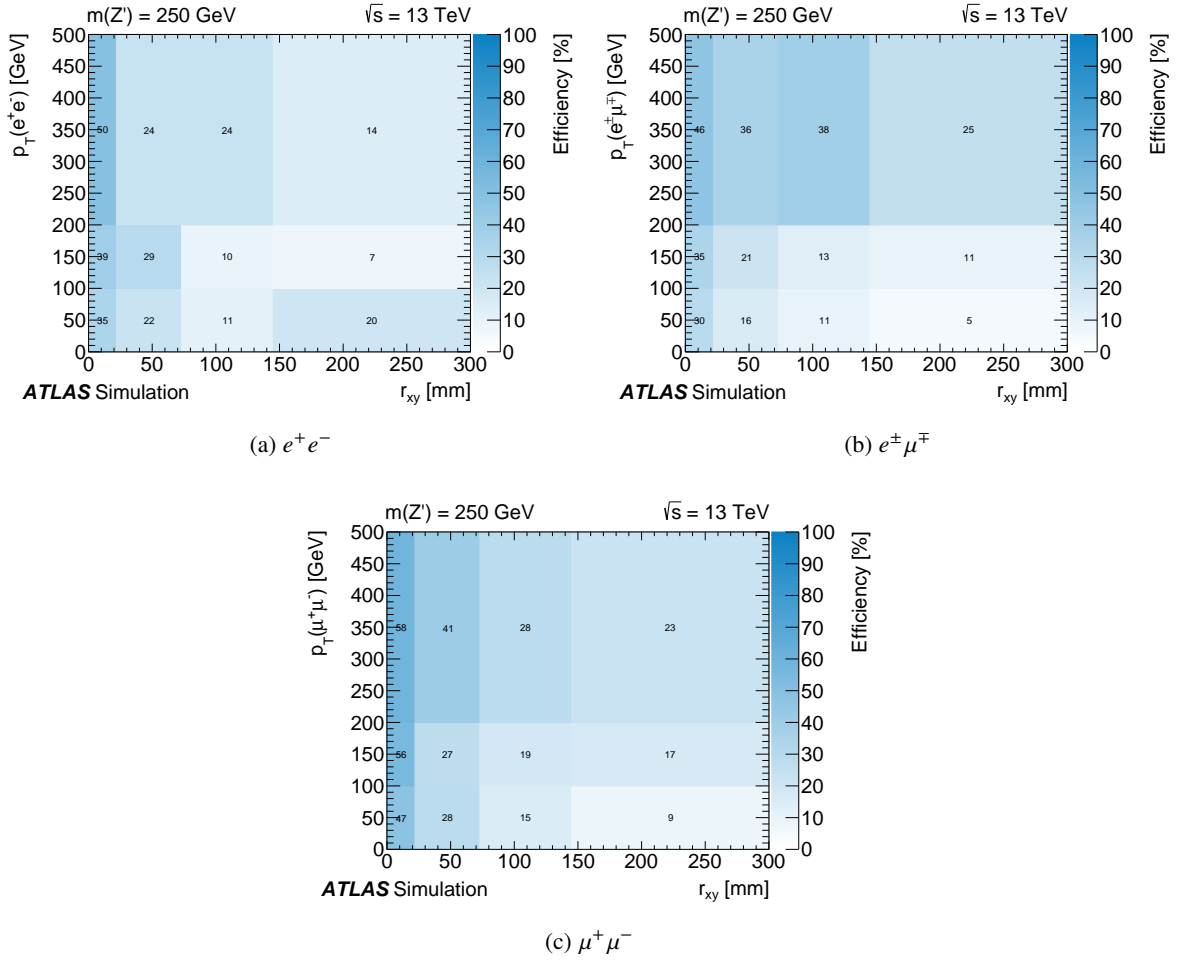


Figure 7: Detection efficiency ϵ per decay as a function of the transverse decay radius r_{xy} and the dilepton p_T for a LLP mass of 250 GeV and (a) $\text{LLP} \rightarrow e^+e^-$, (b) $\text{LLP} \rightarrow e^\pm\mu^\mp$, and (c) $\text{LLP} \rightarrow \mu^+\mu^-$.

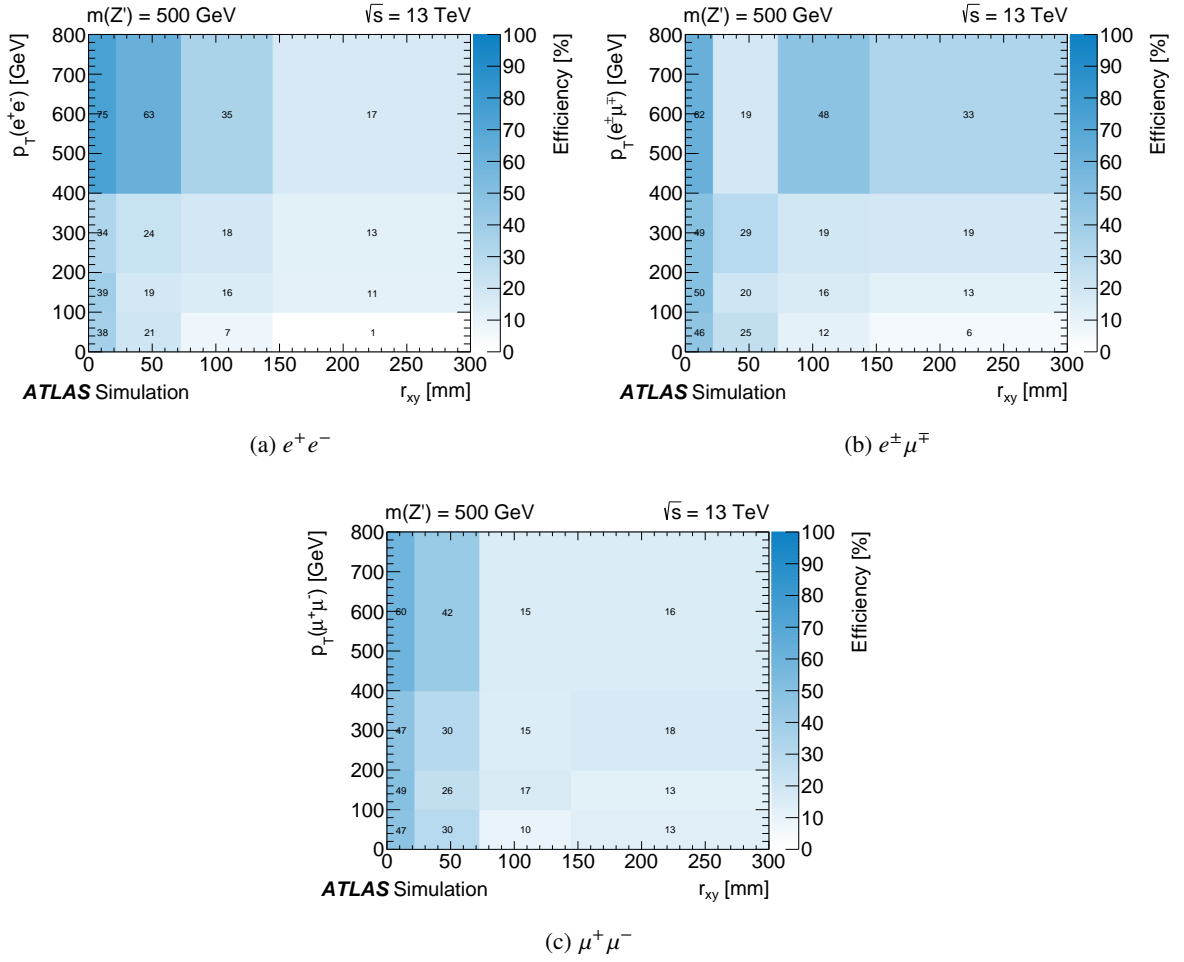


Figure 8: Detection efficiency ϵ per decay as a function of the transverse decay radius r_{xy} and the dilepton p_T for a LLP mass of 500 GeV and (a) $LLP \rightarrow e^+e^-$, (b) $LLP \rightarrow e^\pm\mu^\mp$, and (c) $LLP \rightarrow \mu^+\mu^-$.

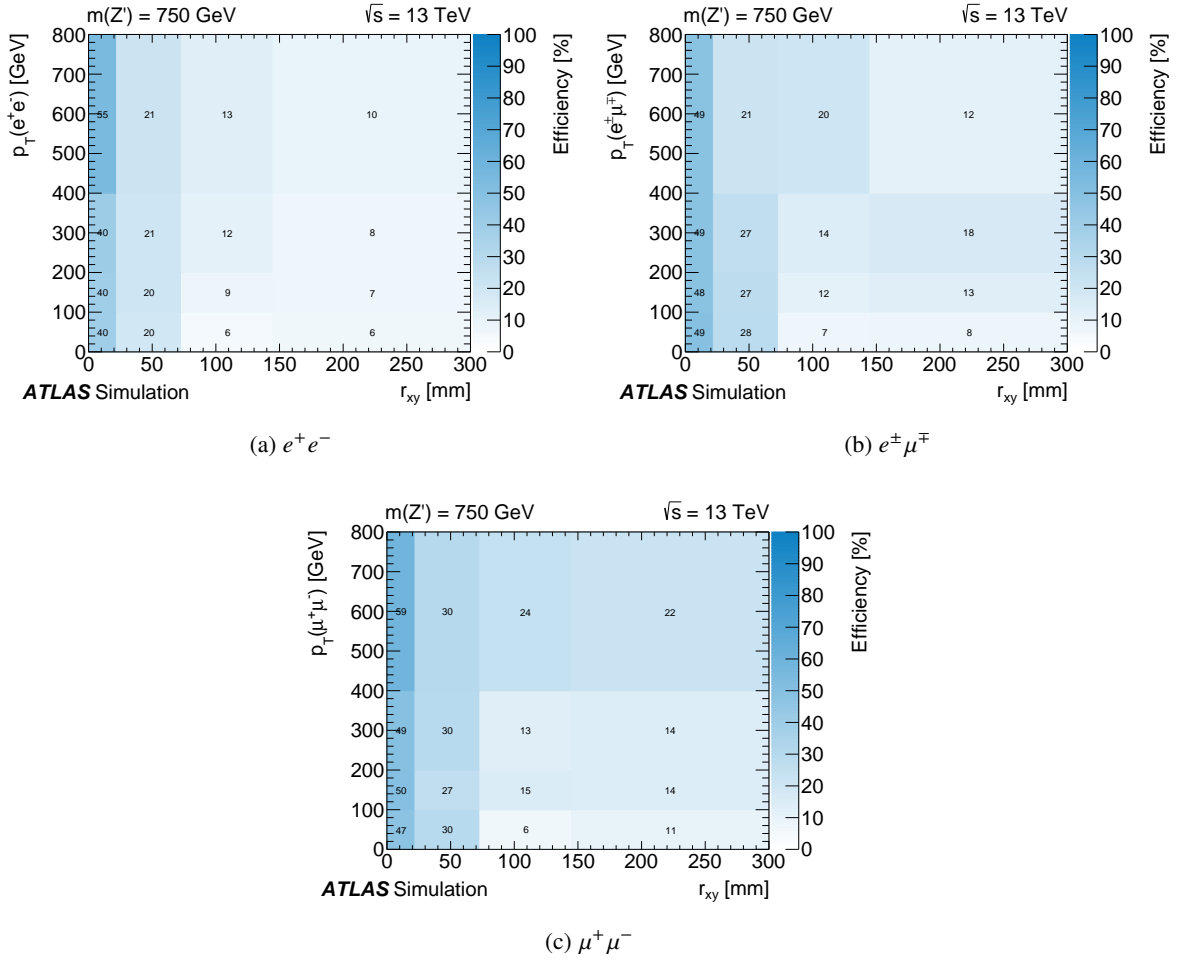


Figure 9: Detection efficiency ϵ per decay as a function of the transverse decay radius r_{xy} and the dilepton p_T for a LLP mass of 750 GeV and (a) $\text{LLP} \rightarrow e^+e^-$, (b) $\text{LLP} \rightarrow e^\pm\mu^\mp$, and (c) $\text{LLP} \rightarrow \mu^+\mu^-$.

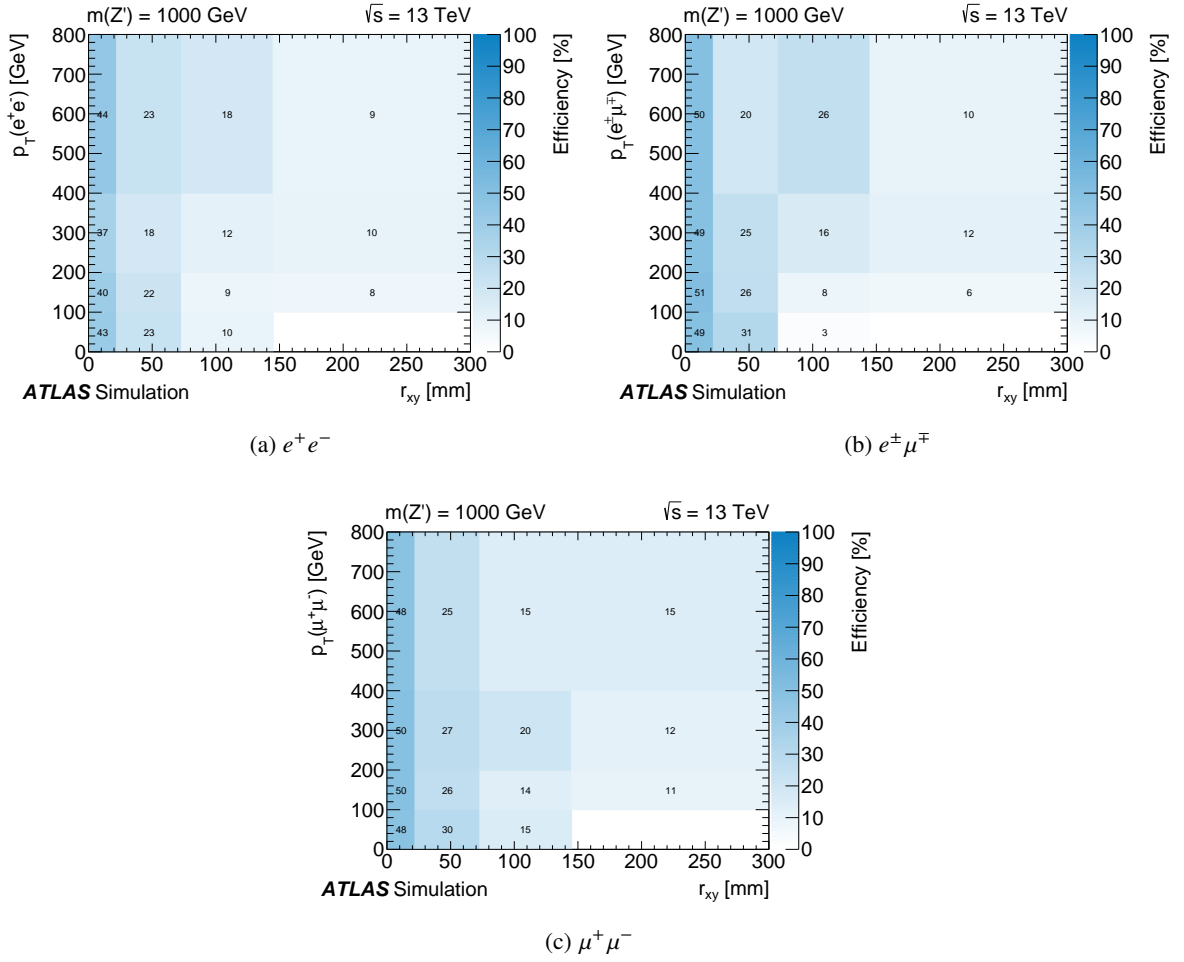


Figure 10: Detection efficiency ϵ per decay as a function of the transverse decay radius r_{xy} and the dilepton p_T for a LLP mass of 1000 GeV and (a) $\text{LLP} \rightarrow e^+e^-$, (b) $\text{LLP} \rightarrow e^\pm\mu^\mp$, and (c) $\text{LLP} \rightarrow \mu^+\mu^-$.